Letter

Antiferromagnetic behavior in self-bound one-dimensional composite bosons

M. C. Gordillo [*]

Departamento de Sistemas Físicos, Químicos y Naturales, Universidad Pablo de Olavide, Carretera de Utrera km 1, E-41013 Sevilla, Spain
and Instituto Carlos I de Física Teórica y Computacional, Universidad de Granada, E-18071 Granada, Spain

(Received 2 January 2024; revised 1 March 2024; accepted 21 May 2024; published 5 June 2024)

The structure of self-bound one-dimensional droplets containing a mixture of ytterbium fermionic isotopes (^{173}Yb, ^{171}Yb) is calculated by means of a diffusion Monte Carlo technique. We considered only balanced setups in which all the atoms of one isotope are spin polarized, while the atoms of the other can have up to three different spin values. Our results indicate that these droplets consist of consecutive "molecules" made up of one ^{173}Yb and one ^{171}Yb atom. The fermionic nature of those Yb atoms makes pairs with identical spin composition avoid each other, producing an effective antiferromagnetic coupling between different kinds of composite bosons. This antiferromagnetism is different than the one induced by an external optical lattice potential within the framework of the Hubbard model reported in previous literature, and different from the standard ferromagnetic behavior typical of bosonic arrangements.

DOI: 10.1103/PhysRevA.109.L061301

The study of self-bound Bose-Bose droplets can be traced to a seminal paper by Petrov [1] that suggested that binary bosonic arrangements with both attractive and repulsive interactions could avoid collapse due to purely quantum effects. Petrov's conclusions gained substantial support through the experimental realization of these droplets [2–5], and originated an extensive body of theoretical work on such systems (see, for instance, Refs. [6,7] and references therein). An obvious follow-up to this line of research is the consideration of Bose-Fermi ensembles, already stable in the mean-field picture [8–12]. Recent experimental work attests to the very rich phase diagram of those Bose-Fermi composite systems [13].

The next logical step involves the exploration of Fermi droplets. Focusing specifically on cold atom systems with only short-range attractive interactions in strictly one-dimensional (1D) environments, to have an stable droplet we would need atoms of at least two different spin types. The problem is that under such circumstances, these atoms pair up to form bosonic molecules that repel each other due to the dual Pauli avoidance exhibited by fermions within a pair with respect to their counterparts with the same spin in other molecules [14,15]. That repulsion makes the molecules separate until their effective interaction is zero. So a set of balanced (with the same number) spin-up and spin-down 1D fermions cannot be self-bound.

In spite of that, there is a way to produce 1D Fermi self-bound drops. The recipe implies to have atoms with at least three different spin flavors, as have been proved to work in small clusters with mixtures of fermionic ytterbium (^{173}Yb and ^{171}Yb) isotopes [15]. We will show that in those systems, the attractive interactions between atoms of different isotopes produce as many kinds of bosonic molecules as the different spin combinations we can assemble to create them. Thus, the Pauli-like avoidance between identical composite bosons creates an effective antiferromagnetic interaction that depends exclusively on the nature of the units formed, not being engineered via an external potential as in previously considered Bose systems loaded in 1D optical lattices and described by a Hubbard model or one of its extensions [16–18]. In that last case, the antiferromagnetic interactions appear only for particular values of the parameters that define the model. Since the Hubbard Hamiltonian is itself an approximation strictly valid only for deep potential lattices, the possibility indicated in this Letter is more general.

The 1D clusters in this Letter will be described by the continuous Hamiltonian [15,19,20],

$$
\begin{aligned}
H = {} & \sum_{i=1}^{N_p} \frac{-\hbar^2}{2m}\nabla_i^2 + g_{\mathrm{1D}}^{173-171}\sum_{i=1}^{N_{173}}\sum_{j=1}^{N_{171}}\delta\left(x_i^{173}-x_j^{171}\right) \\
& + g_{\mathrm{1D}}^{173-173}\sum_{b>a}\sum_{i=1}^{n_{173,a}}\sum_{j=1}^{n_{173,b}}\delta\left(x_{a,i}^{173}-x_{b,j}^{173}\right) \\
& + g_{\mathrm{1D}}^{171-171}\sum_{b>a}\sum_{i=1}^{n_{171,a}}\sum_{j=1}^{n_{171,b}}\delta\left(x_{a,i}^{171}-x_{b,j}^{171}\right),
\end{aligned}
\tag{1}
$$

where N_p is the total number of fermions, while N_{173} and N_{171} are the total number of ^{173}Yb and ^{171}Yb atoms. In this work, $N_{173} = N_{171} = N_p/2$. m is the mass of the atoms, judged to be close enough in both isotopes to be described by a single parameter. No confining external potential in the x direction was imposed. $n_{173,ab}$ and $n_{171,ab}$ are the number of atoms with spins a and b. Identical fermions avoid each other by Pauli's exclusion principle. The g_{1D} parameters depend on the 1D scattering lengths a_{1D} via $g_{\mathrm{1D}}^{\alpha,\beta} = -2\hbar^2/ma_{\mathrm{1D}}(\alpha,\beta)$, with a_{1D}

---

[*] cgorbar@upo.es

defined by [21]

$$a_{1\mathrm{D}}(\alpha,\beta) = -\frac{\sigma_\perp^2}{a_{3\mathrm{D}}(\alpha,\beta)}\left(1 - A\frac{a_{3\mathrm{D}}(\alpha,\beta)}{\sigma_\perp}\right), \qquad (2)$$

with $A = 1.0326$ and $(\alpha,\beta) = (173, 171)$. $\sigma_\perp = \sqrt{\hbar/m\omega_\perp}$ is the oscillator length in the transversal direction, depending on the transversal confinement frequency $\omega_\perp$ taken to be in the range $2\pi\ \times$ 40–100 kHz, tight enough to produce a quasi-one-dimensional system. $a_{3\mathrm{D}}(\alpha,\beta)$ are the three-dimensional experimental scattering lengths between isotopes [22]. The nature of the interactions depends on the sign of those $a_{3\mathrm{D}}$'s: attractive for the ^{173}Yb-^{171}Yb and ^{171}Yb-^{171}Yb pairs and repulsive in the ^{173}Yb-^{173}Yb case.

To solve the Schrödinger equation derived from the Hamiltonian in Eq. (1), we used the fixed-node diffusion Monte Carlo (FN-DMC) algorithm, that gives us the exact ground state ($T = 0$, no excitations) of a 1D system of fermions [23,24] starting from an initial approximation to the exact wave function. Following Refs. [15,19,20], we used

$$\begin{aligned}\Phi(x_1,\ldots,x_{N_p}) &= \mathcal{A}[\phi(r_{11'})\phi(r_{22'})\cdots\phi(r_{N_{173},N_{171}})]\\ &\times \prod_{b>a}\prod_{i=1}^{n_{173,a}}\prod_{j=1}^{n_{173,b}}\frac{\psi\left(x_{a,i}^{173}-x_{b,j}^{173}\right)}{\left(x_{a,i}^{173}-x_{b,j}^{173}\right)}\\ &\times \prod_{b>a}\prod_{i=1}^{n_{171,a}}\prod_{j=1}^{n_{171,b}}\frac{\psi\left(x_{a,i}^{171}-x_{b,j}^{171}\right)}{\left(x_{a,i}^{171}-x_{b,j}^{171}\right)},\end{aligned} \qquad (3)$$

where $\mathcal{A}[\phi(r_{11'})\phi(r_{22'})\cdots\phi(r_{N_{173},N_{171}})]$ is the determinant of a square matrix whose dimension is $N_{173}\times N_{171}$ [25] and takes care of the interactions between pairs of particles of different isotopes separated a distance r_{ij}. The terms $(x_{a,i}^\alpha - x_{b,j}^\alpha)$ in the denominator of Eq. (3) correct the spurious nodes between atoms of the same isotope with different spins (see Refs. [15,19] for further details). $\phi(r_{ij'})$'s are the solutions of the Schrödinger equation for a pair of 1D particles interacting via an attractive delta potential [26],

$$\phi\left(\left|x_i^{173}-x_{j'}^{171}\right|\right) = \exp\left[-\frac{\left|g_{1D}^{173,171}\right|}{2}\left|x_i^{173}-x_{j'}^{171}\right|\right]. \qquad (4)$$

On the other hand, $\psi(x_{a,i}^\alpha - x_{b,j}^\alpha)$'s are Jastrow functions that introduce the correlations between pairs of particles of the same isotope belonging to different spin species a, b. For the repulsively interacting ^{173}Yb-^{173}Yb pair, we have [27]

$$\psi\left(x_{a,i}^{173}-x_{b,j}^{173}\right) = \cos\left(k\left[\left|x_{a,i}^{173}-x_{b,j}^{173}\right| - R_m\right]\right), \qquad (5)$$

when the distance between atoms, $|x_{a,i}^{173}-x_{b,j}^{173}|$, was smaller than a variationally obtained parameter, R_m, and 1 otherwise, k being the solution of the transcendental equation $ka_{1\mathrm{D}}(173,173)\tan(kR_m) = 1$. When the pair of particles of the same isotope attract each other, as in the ^{171}Yb-^{171}Yb case, the Jastrow has the form of Eq. (4) [19,27], but with a different value of the defining constant, $g_{1\mathrm{D}}^{171,171}$.

In this work, we considered 1D arrangements with N_p in the range 16–48. This means $N_{171} = N_{173}$ going from 8 to 24. We have chosen clusters that contain up to three different spin types for ^{173}Yb (out of six available), and up to two for ^{171}Yb (all the possible types for this fermionic isotope). In all cases, one of the Yb isotopes, the majority component, was spin polarized. That those clusters are stable irrespectively of their spin composition can be shown in Fig. 1: The energy per atom is displayed as a function of $|g_{1\mathrm{D}}^{173-171}|$, that depends on the transverse confinement via Eq. (2). We can see that the energy per particle is always lower (more negative) than the corresponding to a set of identical bosonic pairs, $E_b/2 = (g_{1\mathrm{D}}^{173,171})^2/(8\hbar\omega_\perp\sigma_\perp)$ [26]. In that case, the pairs behave as a set of hard bodies due to the double avoidance of the two atoms of the molecule of the same kind of atoms in other pairs. This means that the molecules separate from each other until the interaction *between* molecules is zero.

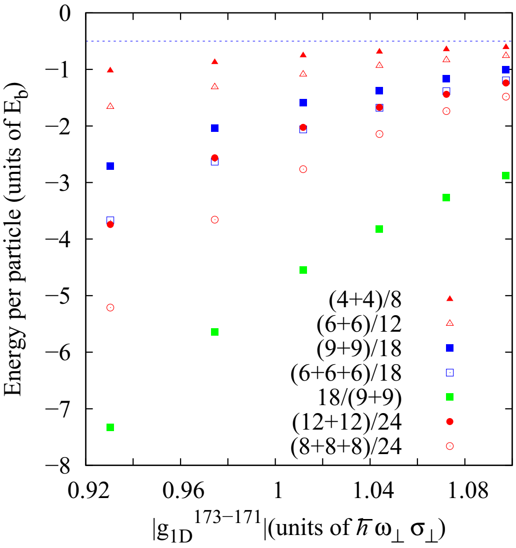

FIG. 1. Energy per Yb atom in units of E_b for balanced clusters with different compositions. The clusters are named as $(\sum_{a=1}^{s173} n_{173,a})/(\sum_{b=1}^{s171} n_{171,b})$, with s the number of spin types. The error bars are of the size of the symbols and not shown for simplicity. The dashed line corresponds to a set of noninteracting ^{173}Yb-^{171}Yb molecules. The range of the $|g_{1\mathrm{D}}|$ parameters corresponds to the range of $\omega_\perp$ and can be deduced from them via Eq. (2).

However, for nonidentical pairs, there is a relaxation of the Pauli's restrictions between atoms of the same isotope and different spins belonging to different ytterbium molecules. This makes those different molecules attract each other, producing the self-bound droplets. When the spin-polarized component is ^{171}Yb, we have to add to the total count of the cluster energy, the repulsive interaction between ^{173}Yb atoms of different spins. That repulsion increases with the transverse confinement (see Ref. [15]), and decreases the binding energy of the entire cluster. On the other hand, when the majority component is ^{173}Yb, there is a residual attraction between the spin-up and spin-down atoms of the ^{171}Yb, being that the interaction is basically constant with $\omega_\perp$ (see again Ref. [15]). However, that energy gets smaller and smaller in comparison to E_b, and hence the shape of the energy of those clusters displayed in Fig. 1. In all cases, we have checked that the molecules formed are stable with respect to thermal excitations at the temperatures used in the experiments: For $\omega_\perp = 2\pi\ \times$ 100 Hz, $E_b \sim$ 1200 nK, an order of magnitude larger than the ~90 nK of the experimental setup in Ref. [28]. Since the energies displayed

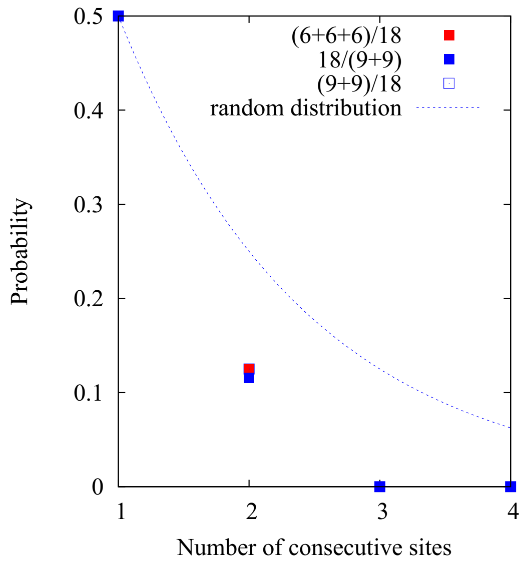

FIG. 2. Probability of having j consecutive sites occupied by atoms of the majority component for clusters of different compositions. Symbols, simulation results; dotted line, values for those probabilities in a random distribution. Error bars are of the size of the symbols and not shown for simplicity.

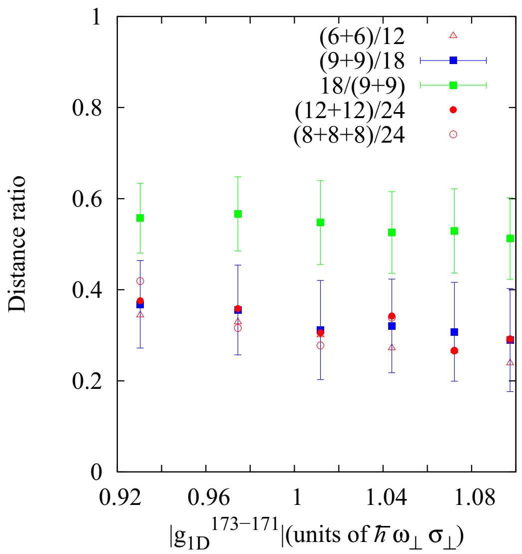

FIG. 3. Ratio between the distances between consecutive $(i, i+1)$ and $(i+1, i+2)$ pairs with i odd for clusters of different compositions as a function of the $|g_{1D}^{173-171}|$ parameter. See further explanation in the text.

in Fig. 1 are of the order of E_b, this also implies that those clusters can be stable under typical experimental conditions. Moreover, the fact that the energy per particle is more negative for larger clusters [compare the values for the $(4+4)/8$ and $(6+6)/12$, for instance] makes them stable with respect to splitting into smaller units.

The next step will be to study the actual distribution of the Yb atoms in those 1D ensembles. To do so, we started by assigning each atom an index i that corresponds to its relative position in the collection of atoms that form the cluster, i.e., for the atom with the lowest x coordinate we have $i = 1$, the one with the second-to-lowest x gets $i = 2$, and $i = N_p$ for the Yb atom at the end of the 1D row. After that, we introduce the variable n_i that takes the value 1 if the atom with index i belongs to the majority (spin-polarized) component and 0 otherwise. With that parameter, we can build the correlators,

$$c_j = \sum_{i=1}^{N_p-j+1} \prod_{k=0}^{j-1} \frac{n_{i+k}}{N_p - j + 1}, \tag{6}$$

to characterize the atom ordering inside the cluster. c_j can be defined as the probability of having a set of j consecutive majority component atoms. For instance, c_4 is the average of the product $n_i n_{i+1} n_{i+2} n_{i+3}$ for all the possible values of i, divided by the total number of sets of four consecutive positions, $N_p - 3$. The results are given in Fig. 2 for c_1–c_4, c_1 being simply the ratio of the majority to the total number of atoms, i.e., 0.5 for all the arrangements considered in this Letter. We represent there different examples of clusters with $N_p = 36$, but the results for other arrangements are virtually identical to those shown.

From Fig. 2 we can see that the distribution of atoms is far from random and independent of the cluster composition. In particular, it is impossible to have more than two ^{171}Yb (in the first example) close together. In addition, the fact that $c_2 \neq 0$ also implies that we do not have a perfect ordering in which each ^{171}Yb is necessarily followed by a ^{173}Yb atom and vice versa. On the other hand, if we calculate the same correlator, but only for $i = 1$ (not considering the entire sum, only the first term), we find $c_2' = 0$ and the same happens when $i = N_p - 1$. Moreover, if we calculate $c_2' = 0$ for atoms other than in the majority component, we get also c_2' for $i = 1, N_p - 1$, i.e., the first two (and the last two) atoms belong to different isotopes. All of this necessarily implies that the atoms distribute themselves in consecutive ^{173}Yb-^{171}Yb units with different orientations.

Unfortunately, this does not necessarily mean that the atoms will form ^{173}Yb-^{171}Yb (in whatever order) molecules in which the atoms in the pair are closer together than a couple of atoms belonging to different units. To check whether we really have those couples, we have calculated the ratio of the distances for all the consecutive $(i, i+1)$ and $(i+1, i+2)$ pairs with i odd. This means that we divided the distance between the first and second atom in a cluster by the distance between the second and third and so on. The average of those ratios should be smaller than one if $(i, i+1)$ pairs with i odd are formed. This is exactly what we see in Fig. 3 for clusters of different sizes and compositions. Thus, it is safe to say that atoms of different isotopes always pair together to form composite bosons well separated from their adjacent couplets. We can see also that the relative distance between separate molecules depends on the nature of the spin-polarized isotope and not on the size of the cluster nor on the number of spin types. Reasonably enough, we also observe that when the interactions between nonpolarized components are attractive, the distance between molecules decreases and the ratio displayed in Fig. 3 increases, as in the $18/(9+9)$ cluster. To serve as a stick for comparison, the intermolecular distance

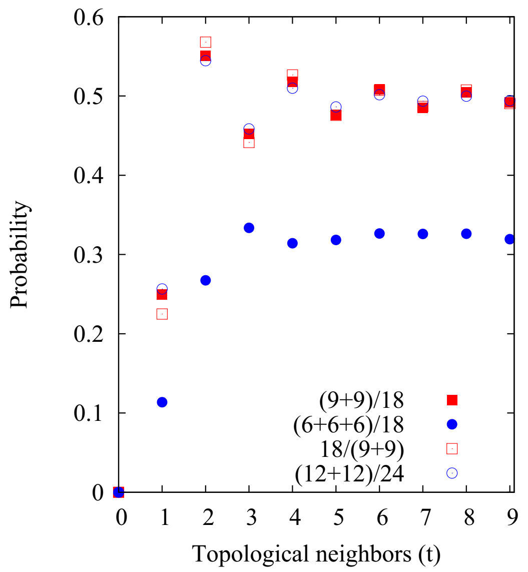

FIG. 4. Probability of having an identical molecule as a tth topological neighbor for clusters of different sizes and compositions. Error bars are of the size of the symbols and not displayed by clarity. Since the majority component is spin polarized, this is equivalent to considering correlations between two equal spins in the minority component as a function of the topological distance.

between the molecules displayed in Fig. 3 ranges in the interval 650–1300 nm.

So far, we have established that all the clusters considered here are made up of molecules consisting of atoms of different isotopes. However, we do not know how those molecules distribute themselves inside the clusters. To address that question, we calculated the probability of having two identical molecules at different topological distances. So, in Fig. 4, nearest neighbors correspond to an abscissa equal to one ($t = 1$), next-to-nearest neighbors to two ($t = 2$), and so on. In a random distribution, that probability is the ratio between the number of pairs of a particular kind to the total number of pairs in the cluster. This means $1/2$ or $1/3$ depending on the number of pair types. In Fig. 4, we can see that the simulation results for several clusters are very close to those values for $t \geqslant 4$. However, the deviations from the random limits are evident for closer neighbors. In particular, there is a “hole” in the probability of having two identical nearest neighbors. This decrease extends to $t = 2$ for clusters with three kinds of molecules. On the other hand, it is more probable to have a next-to-nearest neighbor of the same type than what it would correspond to a random pair ordering. The same can be said of the third neighbor for the $(6 + 6 + 6)/18$ case. This is exactly the same to what happens in all-^{173}Yb fermionic clusters [29] and has its origin in the antiferrromagnetic interactions characteristic of systems of fermions. We have then a set of composite bosons with short-range ($t \leqslant 4$) effective antiferromagnetic interactions.

Summarizing, we have characterized the behavior of strictly 1D clusters of fermionic mixtures of Yb atoms, mixtures that have already been produced experimentally [28,30]. Since the pairing of two fermions produces a boson, the 1D arrangements considered in this work are composite bosons, but with properties derived from their fermionic constituents, in that, they are equivalent to any bosonic atom (for instance, ^{4}He), itself a composite of different fermions. In particular, those composite bosons exhibit a short-range avoidance of identical bosonic molecules. This is completely at odds with the standard ferromagnetic behavior one would expect from a set of regular bosons [16]. In addition, this is an intrinsic behavior that does not depend on a particular choice for the values of the parameters that define the discrete model used to model bosons in an optical lattice, as in reported Ref. [18] and therefore more general.

We acknowledge financial support from Ministerio de Ciencia e Innovación y Universidades MCIN/AEI/10.13039/501100011033 (Spain) under Grant No. PID2020-113565GB-C22 and from Junta de Andalucía group PAIDI-205. We also acknowledge the use of the C3UPO computer facilities at the Universidad Pablo de Olavide.

[1] D. S. Petrov, Quantum mechanical stabilization of a collapsing Bose-Bose mixture, Phys. Rev. Lett. **115**, 155302 (2015).

[2] C. Cabrera, L. Tanzi, J. Sanz, B. Naylor, P. Thomas, P. Cheney, and L. Taurell, Quantum liquid droplets in a mixture of Bose-Einstein condensates, Science **359**, 301 (2018).

[3] P. Cheiney, C. R. Cabrera, J. Sanz, B. Naylor, L. Tanzi, and L. Tarruell, Bright soliton to quantum droplet transition in a mixture of Bose-Einstein condensates, Phys. Rev. Lett. **120**, 135301 (2018).

[4] G. Semeghini, G. Ferioli, L. Masi, C. Mazzinghi, L. Wolswijk, F. Minardi, M. Modugno, G. Modugno, M. Inguscio, and M. Fattori, Self-bound quantum droplets of atomic mixtures in free space, Phys. Rev. Lett. **120**, 235301 (2018).

[5] I. Ferrier-Barbut, H. Kadau, M. Schmitt, M. Wenzel, and T. Pfau, Observation of quantum droplets in a strongly dipolar Bose gas, Phys. Rev. Lett. **116**, 215301 (2016).

[6] F. Böttcher, J.N. Schmidt, J. Hertkorn, K. S. H. Ng, S. D. Graham, M. Guo, T. Langen, and T. Pfau, New states of matter with fine-tuned interactions: quantum droplets and dipolar supersolids, Rep. Prog. Phys. **84**, 012403 (2021).

[7] Z. Luo, W. Pang, B. Liu, Y.Y. Li, and B. A. Malomed, A new form of liquid matter: Quantum droplets, Front. Phys. **16**, 32201 (2021).

[8] L. Salasnich, S. K. Adhikari, and F. Toigo, Self-bound droplet of Bose and Fermi atoms in one dimension: Collective properties in mean-field and Tonks-Girardeau regimes, Phys. Rev. A **75**, 023616 (2007).

[9] M. Tylutki, A. Recati, F. Dalfovo, and S. Stringari, Dark-bright solitons in a superfluid Bose-Fermi mixture, New J. Phys. **18**, 053014 (2016).

[10] D. Rakshit, T. Karpiuk, M. Brewczyk, and M. Gajda, Quantum Bose-Fermi droplets, SciPost Phys. **6**, 079 (2019).

[11] D. Rakshit, T. Karpiuk, P. Zin, M. Brewczyk, M. Lewenstein, and M. Gajda, Self-bound Bose-Fermi liquids in lower dimensions, New J. Phys. **21**, 073027 (2019).

[12] J. C. Peacock, A. Ljepoja, and C. J. Bolech, Quantum coherent states of interacting Bose-Fermi mixtures in one dimension, Phys. Rev. Res. **4**, L022034 (2022).

[13] M. Duda, X. Y. Chen, A. Schindewolf, R. Bause, J. von Milczewski, R. Schmidt, I. Bloch, and X. Luo, Transition from a polaronic condensate to a degenerate Fermi gas of heteronuclear molecules, Nat. Phys. **19**, 720 (2023).

[14] J. N. Fuchs, A. Recati, and W. Zwerger, Exactly solvable model of the BCS-BEC crossover, Phys. Rev. Lett. **93**, 090408 (2004).

[15] M. C. Gordillo, Self-bound clusters of one-dimensional fermionic mixtures, Phys. Rev. Res. **5**, 043144 (2023).

[16] L.-M. Duan, E. Demler, and M. D. Lukin, Controlling spin exchange interactions of ultracold atoms in optical lattices, Phys. Rev. Lett. **91**, 090402 (2003).

[17] S. Trotzky, P. Cheinet, S. Folling, M. Feld, U. Schnorrberger, A. M. Rey, A. Polkovnikov, E. A. Demler, M. D. Lukin, and I. Bloch, Time-resolved observation and control of superexchange interactions with ultracold atoms in optical lattices, Science **319**, 295 (2008).

[18] H. Sun, B. Yang, H. Y. Wang, Z. Y. Zhou, G. X. Su, H. N. Dai, Z. S. Yuan, and J. Pan, Realization of a bosonic antiferromagnet, Nat. Phys. **17**, 990 (2021).

[19] M. C. Gordillo, Pairing in SU(6)×SU(2) one-dimensional fermionic clusters, Phys. Rev. A **102**, 023335 (2020).

[20] M. Gordillo, Metal and insulator states of SU(6)×SU(2) clusters of fermions in one-dimensional optical lattices, New J. Phys. **23**, 063034 (2021).

[21] M. Olshanii, Atomic scattering in the presence of an external confinement and a gas of impenetrable bosons, Phys. Rev. Lett. **81**, 938 (1998).

[22] M. Kitagawa, K. Enomoto, K. Kasa, Y. Takahashi, R. Ciuryło, P. Naidon, and P. S. Julienne, Two-color photoassociation spectroscopy of ytterbium atoms and the precise determinations of s-wave scattering lengths, Phys. Rev. A **77**, 012719 (2008).

[23] B. Hammond, W. A. Lester, and P. Reynolds, *Monte Carlo Methods in Ab Initio Quantum Chemistry* (Wold Scientific, Singapore, 1994).

[24] D. Ceperley, Fermion nodes, J. Stat. Phys. **63**, 1237 (1991).

[25] J. Carlson, S.-Y. Chang, V. R. Pandharipande, and K. E. Schmidt, Superfluid Fermi gases with large scattering length, Phys. Rev. Lett. **91**, 050401 (2003).

[26] D. Griffiths, *Introduction to Quantum Mechanics*, 2nd ed. (Benjamin Cummings, New Jersey, 2004).

[27] G. E. Astrakharchik, Quantum Monte Carlo study of ultracold gases. Ph.D. thesis, Universitá degli Studi Trento, 2004, arXiV:1412.4529.

[28] S. Taie, Y. Takasu, S. Sugawa, R. Yamazaki, T. Tsujimoto, R. Murakami, and Y. Takahashi, Realization of a SU(2) × SU(6) system of fermions in a cold atomic gas, Phys. Rev. Lett. **105**, 190401 (2010).

[29] M. C. Gordillo, F. Mazzanti, and J. Boronat, One-dimensional harmonically confined SU(N) fermions, Phys. Rev. A **100**, 023603 (2019).

[30] B. Abeln, K. Sponselee, M. Diem, N. Pintul, K. Sengstock, and C. Becker, Interorbital interactions in an SU(2)$\bigotimes$SU(6)-symmetric Fermi-Fermi mixture, Phys. Rev. A **103**, 033315 (2021).